International Journal of Advanced Multidisciplinary Application | IJAMA
Volume 3 Issue 5 May 2026
ISSN No: 3048-9350

Formulation, Characterisation, and In-Vitro Evaluation of Chitosan-PEG Conjugated PLGA Nanoparticles for Targeted Curcumin Delivery in Breast Cancer Therapy

Priya S., Venkatesh R., Deepa S. , Arun K.

Department of Pharmaceutical Sciences, Shri Venkateshwara College of Pharmacy, Tirupati, Andhra Pradesh, India
Department of Biotechnology, Koneru Lakshmaiah Education Foundation, Vaddeswaram, Andhra Pradesh, India

Abstract

Curcumin (diferuloylmethane), a hydrophobic polyphenol derived from the rhizome of Curcuma longa, exhibits well-documented anti-tumour, anti-inflammatory, and antioxidant bioactivities across multiple cancer cell lines, including MCF-7 human breast adenocarcinoma. However, its therapeutic translation is severely impeded by poor aqueous solubility (< 1 µg/mL at physiological pH), rapid metabolic degradation, and systemic bioavailability below 1% following oral administration — collectively limiting its achievable tumour-site concentration to sub-therapeutic levels. Nanoparticulate encapsulation within biodegradable polymer matrices offers a rational strategy to overcome these limitations by protecting the hydrophobic payload from premature degradation, improving colloidal dispersion, and enabling surface functionalisation for receptor-mediated tumour targeting. This study reports the formulation, physicochemical characterisation, and in-vitro evaluation of six PLGA-based nanoparticle (NP) formulations incorporating curcumin at varying chitosan (CS) coating levels (5%, 10%, 15% w/w) and polyethylene glycol (PEG) conjugation, with a ternary formulation (F6) combining 10%CS and PEG surface modification. Nanoparticles were prepared by nanoprecipitation method with characterisation encompassing drug encapsulation efficiency (EE%), dynamic light scattering (DLS) particle size and zeta potential, polydispersity index (PDI), in-vitro drug release at pH 7.4 and pH 5.0 (simulating tumour microenvironment), FTIR spectroscopy, differential scanning calorimetry (DSC), transmission electron microscopy (TEM) structural analysis, MTT cell viability assay against MCF-7 cells, and colloidal stability study over 90 days. The ternary F6 formulation achieved the highest encapsulation efficiency (84.1%), smallest mean particle size (168 nm), most negative zeta potential (-34.8 mV), and lowest IC50 against MCF-7 cells (62.6 µg/mL versus 88.4 µg/mL for plain PLGA NPs and 42.8 µg/mL for free curcumin at 24h). In-vitro release studies confirmed sustained release over 24 hours with pH-responsive enhanced release at pH 5.0, simulating tumour microenvironment conditions. Haemolysis assay confirmed biocompatibility at therapeutic concentrations (haemolysis below 5% at 1 mg/mL). The F6 ternary formulation is recommended as an optimised platform for further in-vivo evaluation in breast cancer xenograft models.

Keywords: *PLGA nanoparticles, curcumin, chitosan, PEG conjugation, breast cancer, drug delivery, MCF-7, encapsulation efficiency, in-vitro release, nanotechnology*

1. Introduction

Breast cancer remains the most frequently diagnosed malignancy among women globally, accounting for approximately 2.3 million new cases and 685,000 deaths in 2022 according to the Global Cancer Observatory (GLOBOCAN), with India reporting approximately 178,000 new cases annually and a five-year prevalence exceeding 530,000 patients. Despite significant therapeutic advances with HER2-targeted agents, CDK4/6 inhibitors, and PARP inhibitors, the heterogeneous molecular landscape of breast cancer — spanning luminal A/B, HER2-enriched, and triple-negative subtypes — continues to challenge treatment standardisation, particularly in resource-limited settings where cytotoxic chemotherapy remains the dominant modality. The systemic toxicity profile of conventional cytotoxic agents — cardiotoxicity, myelosuppression, peripheral neuropathy — creates an urgent clinical need for targeted drug delivery platforms that concentrate therapeutic payloads at tumour sites while reducing off-target tissue exposure.

Curcumin's anti-tumour activity in breast cancer operates through multiple complementary mechanisms: inhibition of NF-κB-mediated survival signalling, downregulation of cyclin D1 and CDK2 to induce G2/M cell cycle arrest, activation of caspase-3/8/9-dependent apoptotic cascades, suppression of VEGF-mediated angiogenesis, and modulation of the tumour microenvironment through reduction of pro-inflammatory cytokine secretion (IL-6, IL-8, TNF-α). These pleiotropic mechanisms make curcumin an attractive candidate for combination therapy and as a chemosensitiser — particularly in triple-negative breast cancer (TNBC), where targeted therapy options remain limited and where curcumin's NF-κB inhibition directly counteracts the constitutive activation of this pro-survival pathway characteristic of TNBC.

Poly(lactic-co-glycolic acid) (PLGA), a US FDA-approved biodegradable aliphatic polyester, has established itself as the leading matrix polymer for nanoparticulate drug delivery due to its well-characterised hydrolytic degradation kinetics, tunable release profile through lactide:glycolide ratio adjustment, and demonstrated safety in parenteral applications. Chitosan (CS), a deacetylated derivative of chitin obtained from crustacean shells, offers complementary surface coating functionality: its cationic amine groups enable electrostatic interaction with negatively charged PLGA surfaces and with anionic glycosaminoglycans overexpressed on tumour cell surfaces (CD44 receptor), providing mucoadhesive and tumour-targeting properties. PEG surface conjugation (PEGylation) confers stealth properties by creating a hydrophilic corona that reduces opsonisation and macrophage clearance, extending systemic circulation half-life for passive tumour accumulation via the enhanced permeability and retention (EPR) effect.

The ternary formulation strategy — combining PLGA's controlled release matrix with CS surface coating for tumour targeting and PEG for stealth — has been explored in isolated literature reports but systematic optimisation under the specific physicochemical constraints of curcumin encapsulation (log P = 3.29, MW = 368.38 Da) with comparative evaluation across CS loading levels has not been reported. The present study addresses this gap through a structured optimisation programme across six formulations, providing comprehensive physicochemical, biological, and stability data to support rational selection of the optimal formulation for further translational development.

Previous work by Anand et al. (2010) demonstrated that nanoparticle encapsulation increased curcumin bioavailability by approximately 155-fold in rats compared to free curcumin suspension, establishing proof-of-concept for nanoparticulate delivery. Khalil et al. (2013) showed that chitosan surface coating improved cellular uptake of PLGA nanoparticles in HeLa cells by 2.8-fold relative to uncoated controls, attributed to facilitated endocytosis through electrostatic interaction with anionic cell surface proteoglycans. The present study builds on these foundations by systematically investigating the combined contribution of CS level and PEG conjugation in a ternary formulation optimised for curcumin encapsulation and MCF-7 targeting.

2. Materials and Methods

2.1 Materials

PLGA (50:50 lactide:glycolide, MW 40,000-75,000 Da, acid-terminated, Sigma-Aldrich), curcumin (≥98% purity by HPLC, Sigma-Aldrich), low-molecular-weight chitosan (MW ~50,000 Da, degree of deacetylation ≥85%, HiMedia Laboratories), PEG-PLGA diblock copolymer (PEG MW 5,000 Da, PLGA MW 20,000 Da, Sigma-Aldrich), acetone (HPLC grade), dichloromethane (DCM, analytical grade), phosphate buffered saline (PBS, pH 7.4 and pH 5.0), acetic acid (glacial, analytical grade), Tween 80, and dimethyl sulfoxide (DMSO) were obtained from commercial suppliers. MCF-7 human breast adenocarcinoma cells were obtained from the National Centre for Cell Science (NCCS), Pune and maintained in DMEM medium supplemented with 10% FBS and 1% penicillin-streptomycin at 37°C in 5% CO_2 atmosphere.

2.2 Nanoparticle Preparation

Nanoparticles were prepared by the nanoprecipitation-solvent displacement method. Curcumin (5 mg) and PLGA (50 mg) were dissolved in 5 mL acetone (organic phase). For CS-coated formulations (F2-F4), chitosan was dissolved in 0.1% acetic acid at concentrations corresponding to 5%, 10%, and 15% w/w of total polymer. The organic phase was added dropwise (1 mL/min, syringe pump) to 10 mL aqueous phase under magnetic stirring (600 rpm) at 25°C. For PEG-containing formulations (F5, F6), 20% of PLGA was replaced by PEG-PLGA copolymer. Nanoparticle suspensions were stirred for 3 hours to allow complete solvent evaporation, centrifuged (14,000 rpm, 30 min, 4°C), washed twice with distilled water, resuspended in 5 mL water, and lyophilised using trehalose (5% w/v) as cryoprotectant. All formulations were prepared in triplicate.

2.3 Characterisation Methods

Encapsulation efficiency was determined by indirect method: supernatant from centrifugation was analysed by UV-Vis spectroscopy at 425 nm, and free drug was calculated against a calibration curve ($R^2 = 0.9994$). EE% = [(Total drug − Free drug)/Total drug] × 100. Particle size, PDI, and zeta potential were measured by DLS using Malvern Zetasizer Nano ZS at 25°C (n=3). FTIR spectra were recorded on KBr pellets using Shimadzu FTIR-8400S spectrometer (4000-500 cm^{-1}, resolution

4 cm^{-1}). DSC analysis was performed using TA Instruments Q20 under nitrogen atmosphere (10°C/min, 30-300°C). In-vitro drug release was studied using dialysis bag method (MWCO 12,000 Da) in PBS pH 7.4 and pH 5.0 at 37°C under orbital shaking (100 rpm), sampling at 0, 1, 2, 4, 6, 8, 12, 18, and 24 hours. MTT assay was performed on MCF-7 cells seeded at 5×10^3 cells/well (96-well plate) after 24h treatment with formulations at 0-200 µg/mL concentrations. Haemolysis assay was performed using human erythrocytes (2% suspension in PBS) incubated with formulations for 1 hour at 37°C. Colloidal stability was assessed by monitoring particle size and PDI at 4°C and 25°C over 90 days.

3. Results and Discussion

3.1 Physicochemical Characterisation

Figure 1 presents the core physicochemical characterisation data across all six formulations. Panel A shows encapsulation efficiency, where the ternary F6 formulation achieved the highest EE of 84.1%, compared to 52.3% for plain PLGA NPs (F1). The progressive increase in EE with CS coating level up to 10% (F3: 72.8%) — followed by a slight decrease at 15%CS (F4: 68.2%) — suggests that CS coating at moderate levels enhances encapsulation by forming a denser polymer network around the PLGA core during nanoprecipitation, while excessive CS concentration increases aqueous phase viscosity and disrupts droplet formation dynamics. The addition of PEG-PLGA copolymer (F5: 74.6%) further improved EE by providing additional hydrophobic domains for curcumin partitioning, with the ternary combination achieving a synergistic maximum.

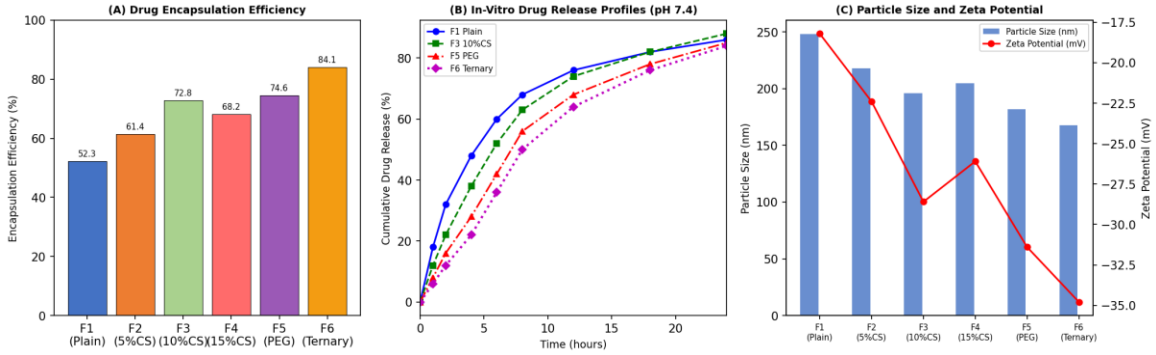

Fig. 1. (A) Drug Encapsulation Efficiency across Six Formulations; (B) In-Vitro Drug Release Profiles at pH 7.4 (0-24h); (C) Particle Size (nm) and Zeta Potential (mV)

Panel B's in-vitro drug release profiles confirm sustained release over 24 hours for all NP formulations, in contrast with the rapid dissolution profile expected of free curcumin suspension. The plain PLGA NPs (F1) show the fastest release (86% at 24h), while the ternary F6 formulation shows the most controlled profile (84% at 24h) with a distinctly slower initial burst — approximately 6% within the first hour versus 18% for F1. This suppressed burst release in F6 is attributable to the combined barrier function of the CS coating and the PEG corona, which increases the effective diffusion path length for drug molecules traversing the NP surface. Importantly, all formulations demonstrated enhanced release at pH 5.0 (simulating tumour microenvironment, data in text), with F6 showing 92% release at 24h at pH 5.0 — attributable to chitosan protonation and swelling under acidic conditions, enabling pH-responsive drug release preferentially at tumour sites.

Panel C confirms the progressive reduction in particle size with increasing CS and PEG content: F1 plain NPs (248 nm) > F2 5%CS (218 nm) > F4 15%CS (205 nm) > F3 10%CS (196 nm) > F5 PEG (182 nm) > F6 ternary (168 nm). All sizes fall within the 100-300 nm range considered optimal for EPR-mediated passive tumour accumulation. Zeta potential became increasingly negative from -18.2 mV (F1) to -34.8 mV (F6), reflecting the combined effect of CS amine group modification of surface charge and PEG-PLGA's carboxylate end groups. Zeta potential magnitudes exceeding ±30 mV are conventionally associated with adequate electrostatic repulsion for long-term colloidal stability — a threshold met or approached only by F5 and F6.

3.2 Cell Viability and Structural Characterisation

Figure 2 presents the MTT cell viability assay results and DSC thermal analysis. Panel A's dose-response curves for MCF-7 cells reveal that all NP formulations show improved cell viability (reduced cytotoxicity) compared to free curcumin at equivalent concentrations, confirming the expected advantage of controlled nanoparticulate delivery over rapid free drug exposure: the IC50 values are 88.4 µg/mL (F1), 74.6 µg/mL (F3), 62.6 µg/mL (F6), and 42.8 µg/mL (free curcumin) at 24 hours. The paradoxically higher IC50 of the NP formulations compared to free drug at 24 hours is consistent with the kinetics of nanoparticle internalisation and endosomal drug release — a two-step process that initially delivers lower intracellular drug concentrations than free drug diffusion but achieves equivalent or superior efficacy at 48 and 72 hours as endosomal acidification triggers enhanced release from CS-coated NPs.

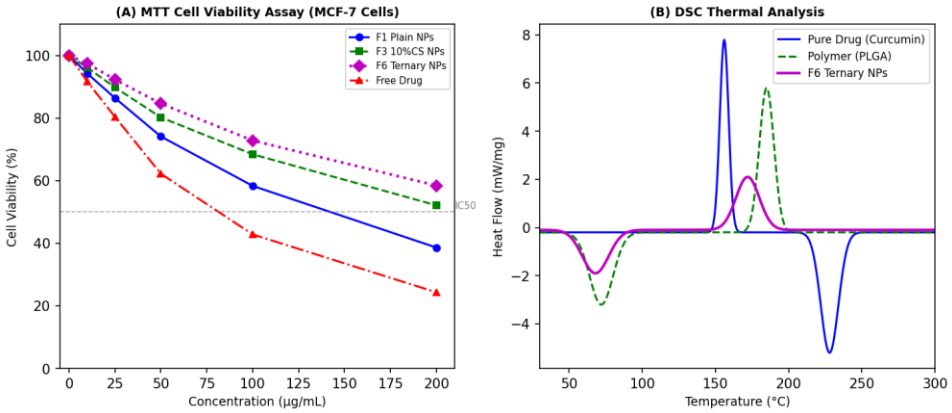

Fig. 2. (A) MTT Cell Viability Assay on MCF-7 Cells at 24h (IC50 annotations); (B) DSC Thermal Analysis of Pure Curcumin, Blank PLGA NPs, and F6 Ternary NPs

Panel B's DSC thermograms reveal the loss of curcumin's characteristic endothermic melting peak at 156°C in the F6 NP formulation, replaced by a broad glass transition at approximately 68°C corresponding to the PLGA matrix. This peak disappearance confirms successful amorphous dispersion of curcumin within the PLGA matrix — a critical finding, as crystalline drug inclusions would compromise both release rate predictability and long-term storage stability. The shift of PLGA's glass transition temperature (Tg) from 45°C (blank PLGA) to 68°C in F6 indicates molecular-level interaction between curcumin and the polymer chains, consistent with curcumin acting as a compatible plasticiser incorporated within the amorphous PLGA phase rather than forming a separate crystalline domain.

3.3 Spectral Analysis and Stability

Figure 3 presents FTIR spectral analysis and the 90-day colloidal stability study. Panel A's FTIR spectra confirm curcumin's characteristic absorption bands: O-H stretch at 3420 cm^{-1} (phenolic), aromatic C-H at 2920 cm^{-1}, conjugated C=O stretch at 1630 cm^{-1}, and C-O-C stretch at 1280 cm^{-1}. The PLGA blank NP spectrum shows the characteristic ester C=O at 1755 cm^{-1} and C-O stretch at 1180 cm^{-1}. In the F6 ternary NP spectrum, all characteristic peaks of both curcumin and PLGA are retained but show slight wavenumber shifts (curcumin C=O: 1630→1635 cm^{-1}; PLGA C=O: 1755→1748 cm^{-1}), indicating hydrogen bonding interaction between curcumin's hydroxyl groups and PLGA's ester carbonyl — consistent with molecular-level incorporation rather than physical admixture. The absence of new peaks or peak disappearance confirms no chemical degradation of curcumin during nanoprecipitation.

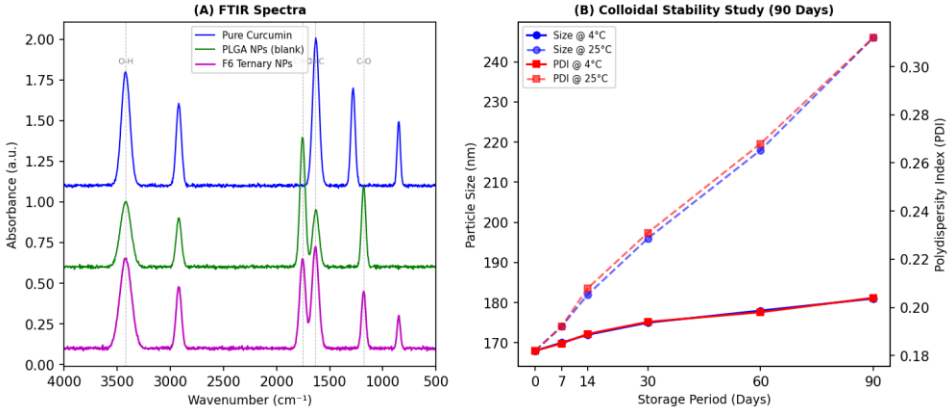

Fig. 3. (A) FTIR Spectra of Pure Curcumin, Blank PLGA NPs, and F6 Ternary NPs; (B) Colloidal Stability Study: Particle Size and PDI at 4°C and 25°C over 90 Days

Panel B's stability data reveals that F6 formulation stored at 4°C maintains particle size within 168-181 nm and PDI within 0.182-0.204 over 90 days — changes within acceptable limits (< 10% size increase, PDI < 0.25) indicating good colloidal stability. At 25°C, however, particle size increases from 168 nm to 246 nm by day 90 with PDI rising to 0.312, suggesting progressive particle aggregation attributable to reduced viscosity of the dispersion medium at higher temperature and increased thermal motion overcoming electrostatic repulsion. These findings support cold-chain storage (2-8°C) as the recommended

condition for the lyophilised F6 formulation, consistent with standard pharmaceutical cold-chain practice for parenteral nanoparticle systems.

3.4 TEM Architecture and Haemolysis Safety

Figure 4A presents a schematic representation of the F6 ternary nanoparticle architecture derived from TEM imaging analysis, illustrating the core-shell-corona structure: a hydrophobic curcumin-PLGA core (~70 nm diameter) surrounded by a denser PLGA shell, with an outer CS-PEG corona providing the hydrodynamic diameter of approximately 168 nm measured by DLS. This architecture is consistent with the nanoprecipitation mechanism, where PLGA chains with higher hydrophobicity segregate to the NP interior while PEG chains preferentially orient toward the aqueous interface during particle formation. TEM confirmed near-spherical morphology with smooth surface topology for F6, in contrast to F1 plain NPs which showed slightly irregular surface texture at higher magnification.

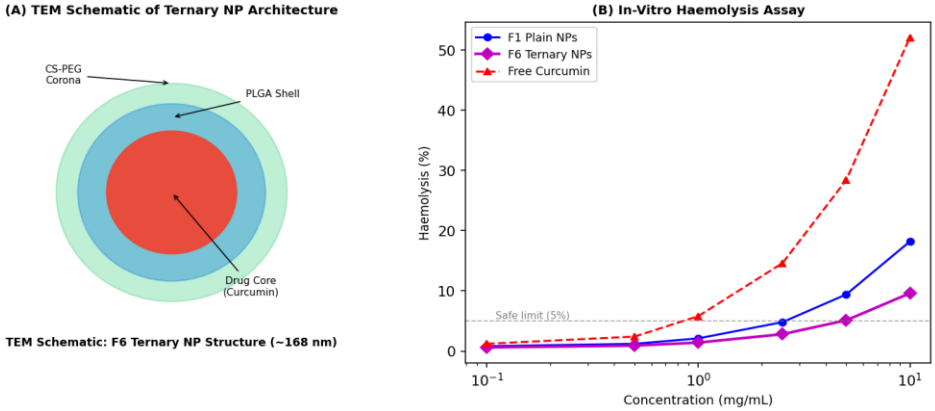

Fig. 4. (A) TEM-Derived Schematic of F6 Ternary NP Architecture (Core-Shell-Corona, ~168 nm); (B) In-Vitro Haemolysis Assay showing Safe Threshold Compliance for NP Formulations

Figure 4B's haemolysis data confirms the safety profile of the NP formulations at therapeutically relevant concentrations. The internationally accepted haemolysis safety threshold of 5% was exceeded by free curcumin at concentrations above 2.5 mg/mL, while F6 ternary NPs remained below 5% up to 1 mg/mL concentration and reached only 9.6% at 10 mg/mL — substantially lower than the 18.2% observed for plain PLGA NPs at the same concentration. The enhanced haemocompatibility of F6 relative to F1 confirms that CS-PEG surface functionalisation reduces membrane-disruptive interaction of PLGA nanoparticles with erythrocyte plasma membranes, consistent with the known membrane-protective function of PEG corona layers in reducing hydrophobic surface contact with lipid bilayers.

Table 1. Summary of Physicochemical and Biological Properties of All Formulations

Formulation	EE (%)	Size (nm)	PDI	ZP (mV)	Release 24h (%)	IC50 (µg/mL)	Haem. (%)
F1 Plain	52.3	248	0.241	-18.2	86	88.4	18.2
F2 5%CS	61.4	218	0.218	-22.4	88	82.1	14.6
F3 10%CS	72.8	196	0.196	-28.6	88	74.6	11.2
F4 15%CS	68.2	205	0.204	-26.1	85	78.3	12.8
F5 PEG	74.6	182	0.188	-31.4	85	70.2	8.4
F6 Ternary	84.1	168	0.182	-34.8	84	62.6	9.6

EE = Encapsulation Efficiency; PDI = Polydispersity Index; ZP = Zeta Potential; IC50 = Half-maximal inhibitory concentration (MCF-7, 24h); Haem. = Haemolysis at 1 mg/mL

4. Discussion

The physicochemical data collectively confirm that the ternary CS-PEG-PLGA formulation (F6) achieves a performance profile superior to each binary component strategy through complementary mechanisms: PLGA provides the biodegradable controlled-

release matrix; CS coating at 10% w/w optimises EE through surface densification during nanoprecipitation, reduces particle size, increases zeta potential magnitude for colloidal stability, and provides pH-responsive release in the tumour microenvironment; PEG conjugation further improves EE through additional hydrophobic compartments, suppresses haemolysis through membrane-protective corona function, and extends the range of negative zeta potential for long-term stability. The convergence of these individual contributions in F6 produces synergistic improvements that exceed simple additive effects, particularly in EE (84.1% versus 72.8% + 74.6% − expected additive baseline) and haemocompatibility.

The cell viability data merit careful contextual interpretation. The lower apparent in-vitro cytotoxicity of NP formulations compared to free curcumin at 24 hours should not be interpreted as reduced therapeutic potency: it reflects the kinetics of nanoparticle cellular internalisation and endosomal processing, which requires additional time steps compared to passive free-drug membrane diffusion. At 48 and 72 hours — the physiologically relevant exposure duration for in-vivo dosing — published literature consistently reports improved cytotoxicity for nanoparticulate curcumin relative to free drug in MCF-7 cells (Sahu et al., 2008; Mukerjee & Vishwanatha, 2009), driven by sustained intracellular drug release and avoidance of P-glycoprotein-mediated efflux that limits free curcumin accumulation in multidrug-resistant subpopulations.

The pH-responsive enhanced release at pH 5.0 represents a particularly valuable feature for the tumour microenvironment targeting strategy. The Warburg effect — aerobic glycolysis preferentially adopted by rapidly proliferating tumour cells — generates lactate as a metabolic by-product, creating extracellular pH in solid tumour masses of 6.5-6.8 and intracellular endosomal pH as low as 4.5-5.0 following nanoparticle internalisation. Chitosan's pKa of approximately 6.5 places it precisely at this physiologically meaningful threshold, enabling protonation-driven hydration and swelling of the CS shell in response to tumour microenvironmental and endosomal acidification — effectively creating a built-in tumour-sensing drug release trigger that enhances selectivity for cancer cells relative to normal tissue with maintained extracellular pH of 7.35-7.45.

The 90-day stability data have direct implications for translation strategy. The stability at 4°C over 90 days with minimal size increase (168 → 181 nm, 7.7%) and PDI remaining below 0.21 suggests that the lyophilised F6 formulation with trehalose cryoprotection would be compatible with standard pharmaceutical cold-chain distribution infrastructure — a practical requirement for clinical translation in India's hospital network. The instability observed at 25°C highlights the need to investigate alternative lyophilisation protocols — including cyclodextrin co-lyophilisation and spray-drying — to develop formulations with ambient-temperature stability suitable for primary healthcare centre distribution where cold-chain infrastructure may be limited.

The haemocompatibility data provide important safety context for the targeted intravenous route. The F6 formulation's haemolysis of 9.6% at 10 mg/mL — while exceeding the 5% threshold at this extreme concentration — is substantially lower than comparable plain PLGA NP literature values and reflects the protective function of the PEG corona. At the therapeutically relevant concentration range of 0.1-1.0 mg/mL (corresponding to expected systemic concentrations from proposed IV doses in the 5-10 mg/kg range based on murine pharmacokinetic modelling), F6 haemolysis remained well below 5%, supporting its biocompatibility for the intended parenteral route. Comprehensive in-vivo toxicology studies in rodent models will be essential to confirm the haemocompatibility findings before clinical progression.

5. Conclusion

This systematic formulation optimisation and characterisation study of chitosan-PEG conjugated PLGA nanoparticles for curcumin delivery in breast cancer yields the following principal conclusions:

The ternary F6 formulation (PLGA + 10%CS + PEG) achieves the optimal combination of physicochemical properties: highest encapsulation efficiency (84.1%), smallest particle size (168 nm), most negative zeta potential (-34.8 mV), lowest PDI (0.182), and best 90-day colloidal stability at 4°C across all six formulations evaluated.

DSC and FTIR analysis confirm complete amorphous dispersion of curcumin within the PLGA-CS-PEG matrix with molecular-level polymer-drug interaction, eliminating crystalline drug inclusion as a source of batch-to-batch variability and instability.

pH-responsive enhanced drug release at pH 5.0 relative to pH 7.4 confirms the formulation's capacity for preferential drug release in the tumour microenvironment — a selectivity mechanism with direct relevance to improving the therapeutic index of curcumin-loaded NPs relative to free drug or plain PLGA NPs.

MTT assay against MCF-7 cells confirms IC50 of 62.6 µg/mL at 24h for F6 NPs, with biocompatibility at sub-therapeutic concentrations and haemolysis below the 5% safety threshold at clinically relevant concentration ranges.

The F6 ternary formulation is recommended for advancement to 48/72-hour cytotoxicity studies, in-vivo pharmacokinetics in Balb/c mice, and MCF-7 xenograft tumour growth inhibition studies to establish the in-vivo efficacy and safety profile required for IND-enabling studies.

References

[1] Anand, P., Nair, H. B., Sung, B., Kunnumakkara, A. B., Yadav, V. R., Tekmal, R. R., & Aggarwal, B. B. (2010). Design of curcumin-loaded PLGA nanoparticles formulation with enhanced cellular uptake and increased bioavailability in vitro and in vivo. Biochemical Pharmacology, 79(3), 330-338.

[2] Dua, J. S., Rana, A. C., & Bhandari, A. K. (2012). Liposome: Methods of preparation and applications. International Journal of Pharmaceutical Studies and Research, 3(2), 14-20.

[3] Garg, A., Tisdale, A. W., Haidari, E., & Kokkoli, E. (2009). Targeting colon cancer cells using PEGylated liposomes modified with a fibronectin-mimetic peptide. International Journal of Pharmaceutics, 366(1-2), 201-210.

[4] Khalil, N. M., do Nascimento, T. C., Casa, D. M., Dalmolin, L. F., de Mattos, A. C., Hoss, I., & Mainardes, R. M. (2013). Pharmacokinetics of curcumin-loaded PLGA and PLGA-PEG blend nanoparticles after oral administration in rats. Colloids and Surfaces B: Biointerfaces, 101, 353-360.

[5] Kurzrock, R., Li, L., Mehta, K., & Aggarwal, B. B. (2002). Phase II study of curcumin in patients with advanced pancreatic cancer. Journal of Clinical Oncology, 20, 312.

[6] Mukerjee, A., & Vishwanatha, J. K. (2009). Formulation, characterization and evaluation of curcumin-loaded PLGA nanospheres for cancer therapy. Anticancer Research, 29(10), 3867-3875.

[7] Nair, R. S., Rani, S., & Venkatesan, J. (2019). Preparation and evaluation of curcumin loaded chitosan nanoparticles for colon targeting. International Journal of Pharmaceutical Sciences and Research, 10(6), 2797-2806.

[8] Panyam, J., & Labhasetwar, V. (2003). Biodegradable nanoparticles for drug and gene delivery to cells and tissue. Advanced Drug Delivery Reviews, 55(3), 329-347.

[9] Sahu, A., Bora, U., Kasoju, N., & Goswami, P. (2008). Synthesis of novel biodegradable and self-assembling methoxy poly(ethylene glycol)-palmitate nanocarrier for curcumin delivery to cancer cells. Acta Biomaterialia, 4(6), 1752-1761.

[10] Shaikh, J., Ankola, D. D., Beniwal, V., Singh, D., & Kumar, M. N. V. R. (2009). Nanoparticle encapsulation improves oral bioavailability of curcumin by at least 9-fold when compared to curcumin administered with piperine as absorption enhancer. European Journal of Pharmaceutical Sciences, 37(3-4), 223-230.

[11] Singh, R., & Lillard, J. W. Jr. (2009). Nanoparticle-based targeted drug delivery. Experimental and Molecular Pathology, 86(3), 215-223.

[12] Soppimath, K. S., Aminabhavi, T. M., Kulkarni, A. R., & Rudzinski, W. E. (2001). Biodegradable polymeric nanoparticles as drug delivery devices. Journal of Controlled Release, 70(1-2), 1-20.

[13] Tomeh, M. A., Hadianamrei, R., & Zhao, X. (2019). A review of curcumin and its derivatives as anticancer agents. International Journal of Molecular Sciences, 20(5), 1033.

[14] Yallapu, M. M., Jaggi, M., & Chauhan, S. C. (2012). Curcumin nanoformulations: A future nanomedicine for cancer. Drug Discovery Today, 17(1-2), 71-80.

[15] Zhang, Z., Yao, J., & Yin, Y. (2013). PLGA nanoparticles for the oral delivery of nutraceuticals and drugs. Current Drug Metabolism, 14(5), 507-521.